Transport description for capture processes in nuclear collisions

S. Ayik
Tennessee Technological University, Cookeville, Tennessee 38505

D. Shapira
Physics Division, Oak Ridge National Laboratory, Oak Ridge, Tennessee 37831

B. Shivakumar
A. W. Wright Nuclear Structure Laboratory, Yale University, New Haven, Connecticut 06511
(Received 28 March 1988)

A transport theory is developed for description of capture processes in low-energy nuclear collisions. It is based on the picture that a dinuclear molecular complex formed during early stages of the collision acts as a doorway configuration toward formation of a fully equilibrated compound nucleus, and this complex can decay into open binary channels while it evolves toward a compound nucleus. The evolution of the dinuclear molecular complex and its decay into binary fragmentation channels are determined by two coupled transport equations. The formalism, in a local equilibrium limit, is successfully applied to analyze complex fragment emission and fusion-evaporation data from collisions of Si+C, Si+N, and Mg+C.

I. INTRODUCTION

Heavy ion collisions at bombarding energies above Coulomb barriers exhibit relaxation processes. These relaxation processes extend continuously from deep inelastic collision (DIC) all the way to compound nucleus formation (CN). DIC occur in collisions for a wide range of initial orbital angular momenta, occupying an angular momentum window between grazing collisions and capture processes (Fig. 1). In collisions with small angular momenta, the projectile and target interpenetrate sufficiently to result in a fully equilibrated CN. The transition between DIC and CN formation takes place smoothly as a function of the orbital angular momentum. For a band of angular momenta in the vicinity of l_{cr} (critical angular momentum for capture), collisions lead to processes which are intermediate between CN formation and DIC. These intermediate processes are characterized by complete energy damping and a broad fragment mass distribution. Measurements of the angular distributions and the kinetic energies of the fragments indicate that the colliding nuclei are captured into a dinuclear molecular complex (DMC) and the observed fragments are emitted from this intermediate stage before going through CN formation.[1-4] The long interaction times associated with the intermediate processes usually lead to the relaxation of the mass-asymmetry mode all the way to symmetric fragmentation. In heavier systems, the intermediate processes are well established and referred to as fast fission or quasifission.[5,6] Similar studies are available for a few light systems (Si+C, Mg+C, Si+N) and these have been referred to as orbiting processes.[7,8]

Statistical descriptions of nuclear collisions, in the framework of transport theories, have been quite successful in understanding the reaction mechanism of DIC. However, these existing transport theories are tailored to study mostly the scattering processes (noncapture processes) and they do not provide a consistent description for the intermediate processes and CN formation[9-14] The intermediate processes involve the formation and evolution of a DMC and its subsequent decay partially by fragmentation and partially by CN formation. Hence, these processes require a consistent description for the evolution of the DMC and its coupling to the compound nuclear states as well as the channel states.

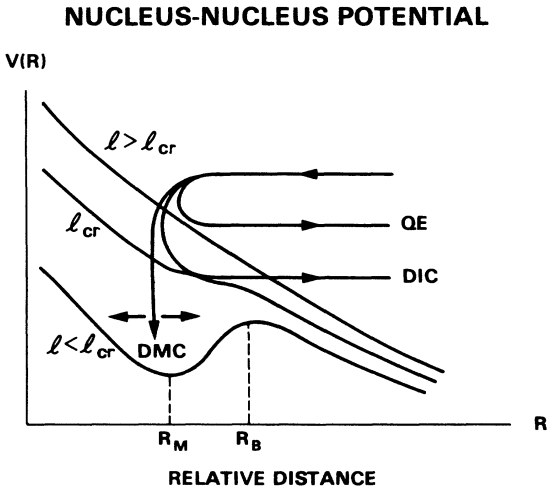

FIG. 1. Typical trajectories of various processes (QE, quasielastic; DIC, deep inelastic; and DMC, dinuclear molecular complex) in low-energy nuclear collisions for different relative angular momenta, l.

In the present work, we develop a transport formalism for nuclear collisions, based on the picture that a DMC is formed during the early stages of the collision.[15–17] It is assumed that as a result of the dissipative forces acting on the relative motion, the colliding ions are trapped into the pocket of the entrance channel nucleus-nucleus potential and a DMC is formed. This DMC acts as a doorway configuration towards formation of a fully equilibrated CN, and it evolves throughout the exchange of nucleons to different dinuclear configurations. At each stage of its evolution, there is a finite probability for direct fragmentation into outgoing channels by dynamical and thermal penetration over the interaction barrier. The doorway states that do not fragment eventually relax into a CN configuration. The evolution of the DMC towards a fully equilibrated CN and its fragmentation into binary exit channels are described by two coupled transport equations for the relevant macroscopic and collective variables of the DMC. The present formalism provides a consistent statistical description for the intermediate processes and CN formation. It allows us to calculate the fragmentation cross section (orbiting yield) and the fusion cross section taking the effects of the entrance channel limitations into account.

In Sec. II the derivation of the coupled transport equations for the evolution of the DMC is presented. In Sec. III a simple model is developed which allows consistent calculation of observables for both fusion and orbiting processes. In Sec. IV the model is applied to the $^{28}Si+^{12}C$ (Refs. 7, and 18–21), $^{28}Si+^{14}N$ (Ref. 8), and $^{24}Mg+^{12}C$ (Refs. 20, 22, and 23) systems. Finally, in Sec. V, the summary and conclusions are given.

II. COUPLED TRANSPORT EQUATIONS

There exist a number of transport theories describing the dissipative processes in DIC.[9–14] However, these theories do not provide a description for the intermediate processes for which the incoming flux can evolve toward a fully equilibrated CN or be emitted back into the binary fragmentation channels. In our description of the capture processes, the existing transport theories are extended by including the coupling of the intermediate doorway states to the compound nuclear states and at the same time to the binary fragmentation channels.

In the early stages of the collision process, a DMC is formed as a result of the trapping of the colliding nuclei in the pocket of the entrance channel nucleus-nucleus potential. It evolves toward a fully equilibrated CN through formation of intermediate doorway states which are metastable bound states of the total system embedded in the continua of the open fragmentation channels.[24] Then, the time-dependent wave function of the system can be expanded in terms of a complete set of intermediate doorway states $|\phi_\lambda\rangle$ and continuum states of channels as

$$|\Psi(t)\rangle=\sum_\lambda a_\lambda(t)|\phi_\lambda\rangle+\sum_j a_j(t)|X_j\rangle \ , \tag{2.1}$$

where $|X_j\rangle$ represents the channel wave functions of the binary fragments determined by the eigenfunctions of the Hamiltonian for the separated fragments. Inserting the expansion (2.1) into the time-dependent Schrödinger equation,

$$i\hbar\frac{\partial}{\partial t}|\Psi(t)\rangle=H|\Psi(t)\rangle \ , \tag{2.2}$$

and assuming that the channel wave functions and the intermediate doorway states are properly orthogonalized, we obtain a set of coupled equations for the occupation amplitudes $a_\lambda(t)$ and $a_j(t)$. The occupation amplitudes for the intermediate doorway states are determined by

$$i\hbar\frac{d}{dt}a_\lambda=\sum_\mu(\epsilon_\lambda\delta_{\lambda\mu}+V_{\lambda\mu})a_\mu+\sum_j V_{\lambda j}a_j \ , \tag{2.3}$$

where ϵ_λ is the energy of the state λ, $V_{\lambda\mu}=\langle\phi_\lambda|H|\phi_\mu\rangle$ is the coupling between different doorway states, and $V_{\lambda j}=\langle\phi_\lambda|H|X_j\rangle$ represent the coupling between doorway states and channel states. The equations for the occupation amplitudes of the channel states are given by

$$i\hbar\frac{d}{dt}a_j=\sum_i(\epsilon_i\delta_{ji}+V_{ji})a_i+\sum_\mu V_{j\mu}a_\mu \ , \tag{2.4}$$

where ϵ_j and $V_{ji}=\langle X_j|H|X_i\rangle$ represent the energies and the coupling matrix elements between channel states, respectively.

The set of coupled equations (2.3) together with (2.4) provides a basis for a microscopic treatment of the collision dynamics. A microscopic treatment requires a detailed description of the intermediate doorway states as well as the coupling between doorway states. Here, we are interested in a description of the gross properties of the collision process. Therefore, we restrict ourselves to a macroscopic treatment within a semiclassical approximation and discuss the statistical aspects of the collision, alone. We assume that the intermediate doorway states $|\phi_\lambda\rangle$ have a dinuclear structure and are characterized by a small set of macroscopic variables such as mass and charge asymmetry defined by the proton and neutron numbers Z,N of one of the partners, distance between two centers R, and neck variable σ. The intermediate doorway states are coupled through a one-body nucleon exchange mechanism. The DMC formed during the early stages of the collision evolves in time populating different dinuclear configurations by mutual exchange of nucleons.

In order to derive transport equations for describing the time evolution of the relevant macroscopic variables, we follow the usual coarse-graining procedure.[9,10] We define averages over dinuclear states by dividing the total space into subspaces. Each subspace contains all the dinuclear states with the same values of some macroscopic variables D, such as the charge and mass asymmetry Z,N; the distance between two centers and the corresponding momentum R,P; the excitation energy ξ; the Z component of the intrinsic angular momentum M; etc., $D=\{Z,N,R,P,\xi,M,\dots\}$. Accordingly, we define coarse-grained occupation probabilities of the dinuclear states,

$$\Pi(D,t)=\sum_{\lambda\in D}a_\lambda(t)a_\lambda^*(t) \tag{2.5}$$

by summing the microscopic probabilities over subspaces. In a similar fashion, the course-grained fragmentation probabilities for the channel space are defined as

$$P(C,t)=\sum_{j\in C} a_j(t)a_j^*(t)\ , \tag{2.6}$$

where $C=\{Z,N,R,P,\xi,M,\dots\}$ is a set of macroscopic variables (similar to that of the DMC) characterizing the binary fragmentation channels. Using the projection formalism of statistical mechanics, the set of equations for the amplitudes $a_\lambda(t)$ and $a_j(t)$ can be transformed into two sets of coupled transport equations for the course-grained distribution functions (2.5) and (2.6). The derivation of transport equations using the projection formalism is given for DIC in Refs. 9 and 10. In the problem considered here, the procedure is exactly the same, except for the fact that, here, we have two sets of macroscopic variables, one for the channel space and one for the DMC. We, therefore, obtain two coupled equations for the distribution function $\Pi(D,t)$ of the DMC

$$\begin{aligned}\frac{d}{dt}\Pi(D,t)=&\int_0^t d\tau\sum_{D'}K_{DD'}(t,\tau)[\rho(D)\Pi(D',t-\tau)-\rho(D')\Pi(D,t-\tau)]\\&-\int_0^t d\tau\sum_{C}K_{DC}(t,\tau)[\rho(C)\Pi(D,t-\tau)-\rho(D)P(C,t-\tau)]\end{aligned} \tag{2.7}$$

and for the fragmentation probability $P(C,t)$,

$$\begin{aligned}\frac{d}{dt}P(C,t)=&\int_0^t d\tau\sum_{C'}K_{CC'}(t,\tau)[\rho(C)P(C',t-\tau)-\rho(C')P(C,t-\tau)]\\&+\int_0^t d\tau\sum_{D}K_{DC}(t,\tau)[\rho(C)\Pi(D,t-\tau)-\rho(D)P(C,t-\tau)]\ .\end{aligned} \tag{2.8}$$

Here $\rho(D)$ and $\rho(C)$ are the density of states of the DMC and the fragmentation channels with fixed values of macroscopic variables D and C, respectively. The collision kernels $K_{DD'}$, $K_{CC'}$, and K_{DC} describe the coupling between dinuclear states, the coupling between fragmentation channels and the coupling between dinuclear states and channels, respectively. Since we are mainly interested in the evolution of mass and charge asymmetry, these transport equations are reduced by integrating over the collective variables R and P for simplicity. As a result, the coupling matrix elements, $V_{\lambda\mu}(t)=V_{\lambda\mu}(R)$, $V_{\lambda j}(t)=V_{\lambda j}(R)$, and $V_{ji}(t)=V_{ji}(R)$, in the collision kernels depend on time through the mean value of relative distance $R(t)$. In Eq. (2.7), the right-hand side consists of gain terms which correspond to transitions from all the dinuclear states with $D\neq D'$ and from all the channel states into the dinuclear states D (first and fourth terms); and loss terms which describe transitions from the dinuclear states D into the other dinuclear states and the channel states (second and third terms). The rate of change of the distribution function $\Pi(D,t)$ is determined by the balance between the gain terms and the loss terms. In a similar way, the rate of change of the fragmentation probability $P(C,t)$ is determined by the balance between the gain terms due to transitions from all the channels with $C\neq C'$ and from all the dinuclear states into the channels C, and the loss terms due to transitions from the channels C into the other channels and the dinuclear states. Equations (2.7) and (2.8) carry memory effects due to the fact that the collision terms are nonlocal in time. The changes of the distribution functions $P(C,t)$ and $\Pi(D,t)$ at time t depend on the past history of the evolution.

The coupled equations (2.7) and (2.8) are in principle exact, and they provide a basis for introducing further approximations. The essential point in deriving a transport equation is based on the assumption that the time scales associated with the macroscopic variables and the collective variables are much longer than the time scale associated with the intrinsic variables. As a result, the intrinsic variables equilibrate fast and remain close to a local equilibrium and the reaction exhibits relaxation processes. The collision terms in (2.7) and (2.8) can be evaluated explicitly by introducing statistical approximations for the coupling matrix elements $V_{\lambda\mu}(t)$, $V_{ji}(t)$, and $V_{\lambda j}(t)$. Here, we consider them in a weak-coupling approximation. In this limit, the collision kernels are given by[11,12]

$$\begin{aligned}K_{DD'}(t,\tau)=&\frac{1}{\hbar^2}\langle V_{\lambda\mu}(t)V_{\mu\lambda}(t-\tau)\rangle_{DD'}\\&\times\exp[-i(\epsilon_D-\epsilon_{D'})\tau/\hbar]+\text{c.c.}\ ,\end{aligned} \tag{2.9}$$

$$\begin{aligned}K_{CC'}(t,\tau)=&\frac{1}{\hbar^2}\langle V_{ji}(t)V_{ij}(t-\tau)\rangle_{CC'}\\&\times\exp[-i(\epsilon_C-\epsilon_{C'})\tau/\hbar]+\text{c.c.}\ ,\end{aligned} \tag{2.10}$$

and

$$\begin{aligned}K_{DC}(t,\tau)=&\frac{1}{\hbar^2}\langle V_{\lambda j}(t)V_{j\lambda}(t-\tau)\rangle_{DC}\\&\times\exp[-i(\epsilon_D-\epsilon_{C'})\tau/\hbar]+\text{c.c.}\ ,\end{aligned} \tag{2.11}$$

where $\langle\ \rangle$ denotes the averages over the subspaces. In the weak-coupling limit, the decay times of the collision kernels (memory time) are determined by the correlation time τ_0 of the coupling matrix elements. It is defined by the supposition that the autocorrelation of the matrix elements decays like a Gaussian

$$\langle V_{\lambda\mu}(t)V_{\mu\lambda}(t-\tau)\rangle=\langle V_{\lambda\mu}(t)V_{\mu\lambda}(t)\rangle\exp(-\tau^2/2\tau_0^2) \tag{2.12}$$

and assumed to be the same for all the matrix elements

and independent of the macroscopic variables. For the weak-coupling limit to be valid, the correlation time τ_0 should be the smallest of all the characteristic times of the process. In particular, the correlation time should be much smaller than the relaxation times $\tau(D),\tau(C)$ of the macroscopic variables, $\tau_0 \ll \tau(D),\tau(C)$. Furthermore, in the weak-coupling limit the memory effects can be neglected (Markov approximation).[11,12] The time integrations in Eqs. (2.7) and (2.8) can be done by neglecting the τ dependencies in the distribution functions and we obtain two coupled ordinary transport equations for $\Pi(D,t)$ and $P(C,t)$,

$$\frac{d}{dt}\Pi(D,t)=\sum_{D'} W_{DD'}(t)[\rho(D)\Pi(D',t)-\rho(D')\Pi(D,t)] + \sum_{C}[P(C,t)\Gamma_{C\to D}(t)-\Pi(D,t)\Gamma_{D\to C}(t)] \tag{2.13}$$

and

$$\frac{d}{dt}P(C,t)=\sum_{D}\Pi(D,t)\Gamma_{D\to C}(t) - P(C,t)\sum_{D}\Gamma_{C\to D}(t)\ . \tag{2.14}$$

Here the average transition probability between dinuclear states is given by

$$W_{DD'}=\frac{\sqrt{2\pi}}{\hbar^2}\langle |V_{\lambda\mu}(t)|^2\rangle_{DD'}\tau_0 \times\exp[-(\epsilon_D-\epsilon_{D'})^2\tau_0^2/2\hbar^2] \tag{2.15}$$

and $\Gamma_{D\to C}(t)$, $\Gamma_{C\to D}(t)$ denote the average decay rates for going from a dinuclear state D to a fragmentation channel C, and for the inverse process. The decay rates are given by an average transition probability between dinuclear states and channel states multiplied by the density of the final states,

$$\Gamma_{D\to C}(t)=W_{DC}(t)\rho(C),\quad \Gamma_{C\to D}(t)=W_{DC}(t)\rho(D)\ , \tag{2.16}$$

where the average transition probability is given by

$$W_{DC}(t)=\frac{\sqrt{2\pi}}{\hbar^2}\langle |V_{\lambda j}(t)|^2\rangle_{DC}\tau_0 \times\exp[-(\epsilon_D-\epsilon_C)^2\tau_0^2/2\hbar^2]\ . \tag{2.17}$$

In general, there are additional gain and loss terms in Eq. (2.14) resulting from channel-channel coupling and these contributions are neglected here by assuming that the direct contributions to the binary decays are small.

The coupled transport equations (2.13) and (2.14) provide a unified description for a wide range of relaxation processes observed in nuclear collisions. The underlying reaction mechanism is rather similar to that of preequilibrium particle emission, as illustrated in Fig. 2. As can be seen from this figure, the DMC formed during the early stages of the collision acts as a doorway state for an evolution toward formation of a fully equilibrated CN. The initial DMC evolves in time by exchange of nucleons and by other excitation mechanisms, and different dinuclear configurations are populated as the reaction proceeds. The transport equation (2.13) describes this evolution as a relaxation process in the mass-asymmetry variable and in other macroscopic variables of the DMC. At every stage of the evolution, the DMC can decay into open binary channels by dynamical coupling and at later stages by thermal penetration over the interaction barrier. The decay of the DMC into binary fragments is described by the second transport equation (2.14). The fraction of the incoming flux which results in a fully equilibrated CN (versus the fraction that is emitted back into binary channels) is determined mainly by the angular momentum brought into the system. In collisions with the orbital angular momenta l_{cr} (critical angular momentum for capture), the nucleus-nucleus potential does not exhibit a pocket. Hence, the DMC cannot populate the CN and collisions lead to predominantly DIC processes. On the other hand, in collisions with orbital angular momenta $l \le l_{cr}$, the fraction of the incoming flux results in a CN increases while the fraction emitted back into binary channels decreases with decreasing l due to the fact that the pocket in the nucleus-nucleus potential becomes more and more pronounced. The relative contributions to the CN formation and the binary fragmentation are determined by solving the coupled transport equations (2.13) and (2.14) for each orbital angular momentum. The fully equilibrated CN can decay by particle emission or by fission. The decay of the CN is contained as a special limit of the coupled transport equations (2.13) and (2.14). At the equilibrium limit, the DMC approaches the CN, $\Pi(D,t)\to\Pi(\mathrm{CN},t)$, then the first term in Eq. (2.13) identically vanishes. Furthermore, the decay rate $\Gamma_{C\to D}$ also vanishes, because channels cannot repopulate the CN. As a result, the coupled transport equations become

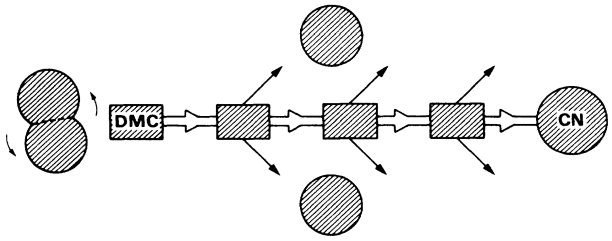

FIG. 2. Illustration of capture processes and compound nucleus formation.

$$\frac{d}{dt}\Pi(\mathrm{CN},t)=-\Pi(\mathrm{CN},t)\sum_{C}\Gamma_{\mathrm{CN}\to C}\ , \tag{2.18}$$

$$\frac{d}{dt}P(C,t)=\Pi(\mathrm{CN},t)\Gamma_{\mathrm{CN}\to C}\ . \tag{2.19}$$

The solution of these equations is trivial, and the decay probability of the CN into the channel C is given by

$$P_{\mathrm{eq}}(C)=\Gamma_{\mathrm{CN}\to C}\Big/\sum_{C}\Gamma_{\mathrm{CN}\to C}\ , \tag{2.20}$$

which is identical to the Hauser-Feshbach formula.

III. ORBITING AND FUSION

In this section, we consider orbiting processes and discuss the applications of the coupled transport equations derived in the previous section, to calculate the orbiting yield and the fusion cross section. As the DMC relaxes towards to a fully equilibrated CN, it can emit binary fragments. The fragmentation probability into a specific channel can be calculated using the solution of the coupled transport equations (2.13) and (2.14),

$$P(C)=\int_0^{t_{\rm eq}} dt \sum_D \Pi(D,t)\Gamma_{D\to C}(t) \times\exp\left[-\int_t^{t_{\rm eq}} dt' \sum_D \Gamma_{C\to D}(t')\right] +P_{\rm eq}(C)\ . \tag{3.1}$$

Here, the first term describes the nonequilibrium fragmentation probability from an initial time until a final time $t_{\rm eq}$ at which the DMC becomes a fully equilibrated CN. The second term describes the fragmentation probability from an equilibrated CN and it is given by (2.20).

Depending on the particular processes under consideration, it is useful to incorporate further approximations in the evaluation of (3.1). Here we consider specifically the orbiting processes in light systems. Studies of orbiting processes, for example, Si+C and Si+N collisions,[7,8] show that the total final kinetic energies of the emitted fragments are fully relaxed and determined by the potential and the rotational energies stored in the DMC. Furthermore, all the fragments have the same $1/\sin\theta$ angular distributions (isotropic emission). These observations indicate that the lifetime of the orbiting complex is sufficiently long and during its lifetime the energy, the angular momentum, and the mass asymmetry of the DMC have reached the equilibrium values. In this case, calculation of the fragmentation probability using (3.1) can be simplified to a large extent. Assuming that the fragments are emitted from a long-lived, equilibrated DMC, the distribution function $\Pi(D,t)$ for each orbital angular momentum l in Eq. (3.1) can be approximated by a constrained equilibrium distribution determined by the potential energy surface of the DMC as

$$\Pi^l_{\rm eq}(D)=\frac{\rho[E-U_l^{\rm min}(N,Z;R,\sigma)]}{\sum_{N,Z}\rho[E-U_l^{\rm min}(N,Z;R,\sigma)]}\ . \tag{3.2}$$

Here ρ is the density of states of the DMC and is calculated at the minimum of the entrance channel potential energy, in the sticking limit. The potential energy surface of the DMC (in the sticking limit), as a function of mass and charge asymmetry (N,Z) and collective variables (R,σ) (R =distance between centers, σ=neck-deformation variable) is given by the sum of nuclear, Coulomb, and rotational energies as

$$U_l(N,Z;R,\sigma)=V_n(N,Z;R,\sigma)+V_C(N,Z;R,\sigma) +\frac{\hbar^2 l(l+1)}{2I_{\rm tot}(N,Z;R,\sigma)}+Q(N,Z)\ , \tag{3.3}$$

where the rotational energy is evaluated with the total moment of inertia $I_{\rm tot}$ of the DMC, and $Q(N,Z)$ is the ground-state Q value of the entrance channel with respect to the fragmentation (N,Z). Furthermore, we approximate the decay rates in (3.1) by their values $\Gamma^l_{D\to C}$ and $\Gamma^l_{C\to D}$ corresponding to the equilibrium shapes of the DMC with fixed (N,Z). Performing the time integration, the binary fragmentation probability for a given orbital angular momentum l can be expressed as

$$P_l(C)=\sum_D \Pi^l_{\rm eq}(D)\Gamma^l_{D\to C}\Big/\sum_D \Gamma_{C\to D}\ . \tag{3.4}$$

A dinuclear state with a mass and charge asymmetry (N,Z) decays predominantly into channels which have a similar value of (N,Z) due to a larger overlap between dinuclear states and channel states. Therefore, the largest contribution to the fragmentation in (3.4) comes from the decay of DMC with $C=D$. Retaining only the diagonal term in (3.4) and using the fact that the decay rates are proportional to the final density of states, we obtain for the fragmentation probability into a channel $C=(N,Z)$ with angular momentum l, a simple result,

$$P_l(N,Z)=\Pi^l_{\rm eq}(N,Z)\cdot\frac{\rho[E-U_l^{\rm sad}(N,Z;R,\sigma)]}{\rho[E-U_l^{\rm min}(N,Z;R,\sigma)]}\ . \tag{3.5}$$

In obtaining this result, the density of the channel states is approximated by the density of dinuclear states at the saddle point (conditional saddle) and the density of dinuclear states is calculated at the minimum of the potential energy surface with fixed (N,Z). The formula (3.5) has a simple interpretation. It contains two factors: the first factor $\Pi^l_{\rm eq}(N,Z)$ gives the probability of finding the DMC with mass and charge asymmetry (N,Z) and it is calculated by (3.2). The second factor gives the escape probability into the fragmentation channel (N,Z) and it is determined by the ratio of the density of states of the DMC at the conditional saddle point and at the minimum of the potential energy surface with fixed (N,Z).

The observable quantities can be calculated using the result (3.5) for the fragmentation probability. The total fragmentation cross section into an exit channel with a product (N,Z) (orbiting yield) is obtained by summing over all the partial waves up to an $l_{\rm max}$,

$$\sigma(N,Z)=\frac{\pi}{k^2}\sum_{l=0}^{l_{\rm max}}(2l+1)P_l(N,Z)\ , \tag{3.6}$$

where $l_{\rm max}$ is the maximum entrance channel angular momentum which leads to a trapping of the colliding nuclei into a DMC. It is determined from the requirements that the trajectory of the relative motion must surmount the entrance channel nucleus-nucleus potential, and furthermore, the potential energy surface must exhibit a pocket. Otherwise, the system cannot be trapped long enough into a DMC and the collision proceeds as a deep inelastic process. The final total kinetic energy $T_l(N,Z)$ of the emitted fragments for each partial wave l is determined by the sum of the potential and the rotational energies at the conditional saddle point,

$$T_l(N,Z)=U_0(N,Z;R_s,\sigma_s)+\frac{\hbar^2 fl(fl+1)}{2I_{\rm rel}(N,Z;R_s,\sigma_s)} , \quad (3.7)$$

where $I_{\rm rel}(N,Z;R_s,\sigma_s)$ is the relative moment of inertia at the saddle point (R_s,σ_s) and sticking is assumed, i.e., $f=I_{\rm rel}(N,Z;R_s,\sigma_s)/I_{\rm tot}(N,Z;R_s,\sigma_s)$. The potential energy $U_0(N,Z;R,\sigma)$ is given by (3.3) with $l=0$. The average kinetic energy of the exit channel can be calculated as

$$T(N,Z)=\frac{\pi}{k^2}\sum_{l=0}^{l_{\max}}(2l+1)T_l(N,Z)/\sigma(N,Z) . \quad (3.8)$$

The dinuclear states, which are not fragmented, must eventually relax into a compound nuclear configuration. In order to calculate the fusion cross section, detailed information about the relaxation of the DMC into a CN is not required. The knowledge of the fragmentation probability (3.5) allows us to calculate the fusion cross section, also. What is not fragmented must end up relaxing into a CN. For each partial wave, the probability for fusion is determined by $1-P_l$, where P_l is the total fragmentation probability obtained by summing over all possible fragmentations,

$$P_l=\sum_{N,Z}P_l(N,Z) . \quad (3.9)$$

Then, the fusion cross section is given as

$$\sigma_f=\frac{\pi}{k^2}\sum_{l=0}^{l_{\max}}(2l+1)(1-P_l) . \quad (3.10)$$

This result together with (3.6) and (3.8) provide a unified and consistent description for the fusion and orbiting processes observed in heavy ion collisions.

IV. APPLICATIONS

We apply the model developed above to describe the fusion and orbiting data measured for the light systems ^{28}Si+^{12}C,[7,18–21] ^{24}Mg+^{12}C,[20,22–23] and ^{28}Si+^{14}N.[8] For these light systems, we expect that the deformation of the DMC will not have an important effect. Therefore, neglecting the neck formation, we represent the equilibrium shape of the DMC for fixed (N,Z) by two rigidly rotating spherical nuclei, with a distance R between their centers. Within this approximation, the fragmentation probability (3.5) takes the form

$$P_l(N,Z)=\frac{\rho[E-U_l(N,Z;R_B)]}{\sum_{N,Z}\rho[E-U_l(N,Z;R_M)]} , \quad (4.1)$$

where the density of states of the DMC ρ are evaluated at the top of the barrier with $R=R_B$ and at the minimum with $R=R_M$, at the entrance channel potential energy. The entrance channel potential energy is given by (3.3), without any neck formation or deformation, $U_l(N,Z;R)=U_l(N,Z;R,\sigma=0)$. For the density of states, we employ the Fermi gas level density expression,

$$\rho[E-U_l(N,Z;R)]=C_l\frac{\exp(2\{a[E-U_l(N,Z;R)-E_p(N,Z)]\}^{1/2})}{[E-U_l(N,Z;R)-E_p(N,Z)]^2} , \quad (4.2)$$

where a is the standard global level density parameter taken as $A/8$ with A as the total mass number of the DMC, $E_p(N,Z)$ is a pairing correction, and C_l is a constant. In the calculation of the potential energy (3.3), we chose for the nuclear potential the empirical proximity potential of Bass.[25] The Q values are obtained from the mass tables and the moments of inertia are approximated by their rigid body values. The Coulomb energies are evaluated as in Ref. 26. The proton and neutron pairing energies for a nucleus of mass number A are given by $\Delta_n=\Delta_p=12\sqrt{A}$ MeV.[27] The pairing corrections $E_p(N,Z)$ in (4.2) are chosen to be equal to the mass weighted mean of the pairing energies of the two nuclei forming the DMC. The density of states for excitation energies below the pairing correction $E_p(N,Z)$ are obtained using a quadratic extrapolation. The empirical Bass potential contains four parameters, $(A,B;d_1,d_2)$, describing the strengths and ranges of a short-range and a long-range proximity potential, respectively. These parameters are determined by a fit to a large amount of fusion data. Their global values are given by $A=0.033$, $B=0.0061$ in terms of MeV^{-1}fm and $d_1=3.3$ fm, $d_2=0.65$ fm. However, the strength parameters A and B exhibit large fluctuations up to 50% for different colliding systems. Therefore, we consider A and B as free parameters and adjust them by fitting the kinetic energies of emitted fragments.

As a first application of the model, we consider the collision of Si+C. Figures 3–5 show the data together with the results of calculations. The data are shown as solid triangles, squares, and circles, and the lines are results of calculations. The maximum angular momentum $l_{\max}(E)$ restricting the summation over partial waves in Eqs. (3.6), (3.8), and (3.10) depends on the bombarding energy and it increases by one unit as the bombarding energy exceeds the corresponding barrier height in the effective potential. As a result, the calculated quantities exhibit discontinuous jumps as a function of bombarding energy. In Fig. 3, the final kinetic energies of the three strongest channels C+Si, N+Al, and O+Mg in a collision of the Si+C system are plotted as a function of center of mass bombarding energy and compared with the measurement. A good description of the kinetic energy spectra is obtained by taking the strength parameter A in the range between 0.045 and 0.050 and the global values obtained by Bass[25] for the other parameters. The results of calculations with $A=0.046$ (set I) and with $A=0.048$ (set II) are shown in part (a) and part (b) of Fig. 3, respectively. Calculation with either set of parameters provides a good description for the final kinetic energies for all the chan-

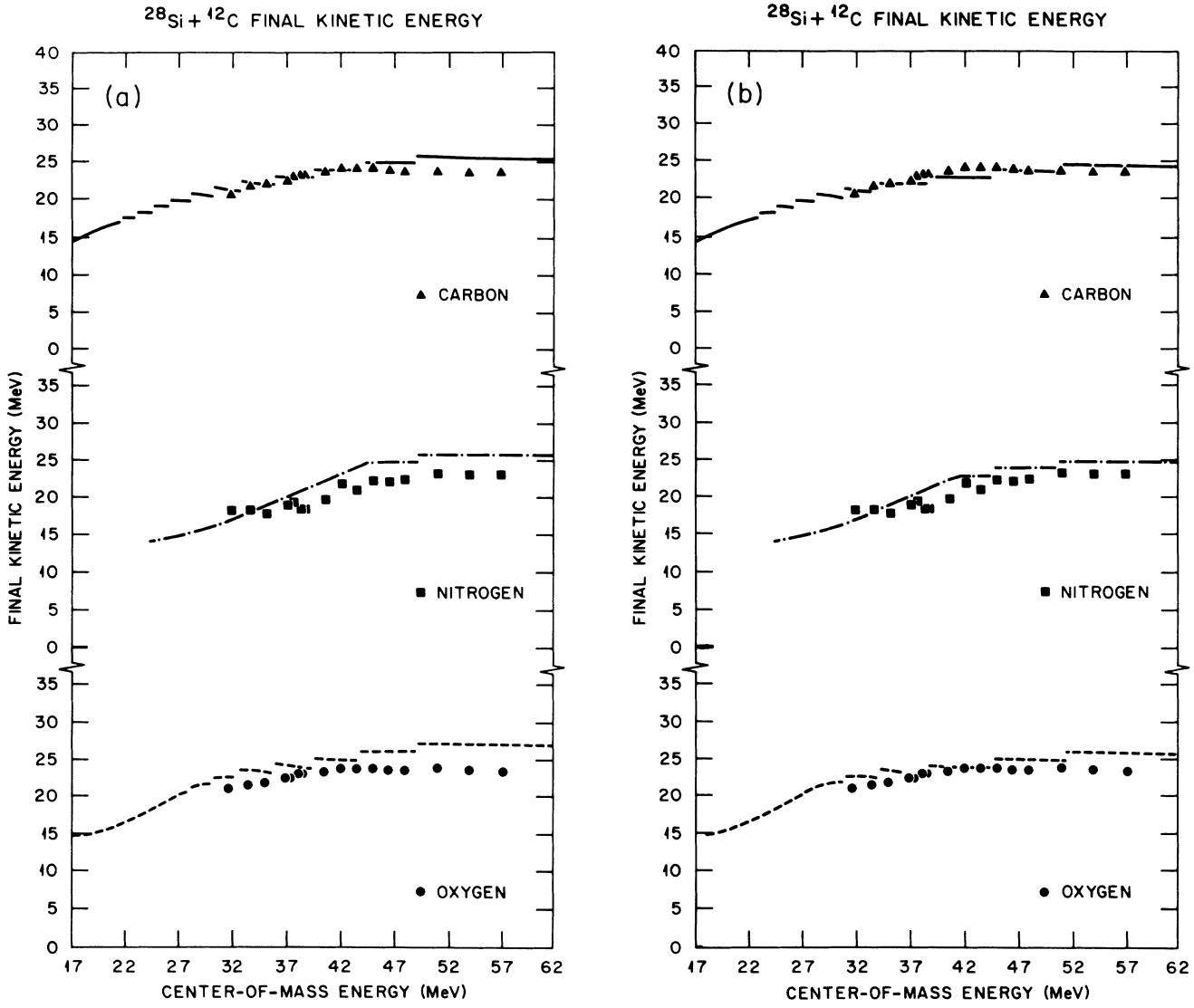

FIG. 3. (a) Measured and calculated (with set I) final kinetic energies of C, N, and O channels in Si+C collisions plotted as functions of bombarding energy. (b) As in part (a), but with parameter set II.

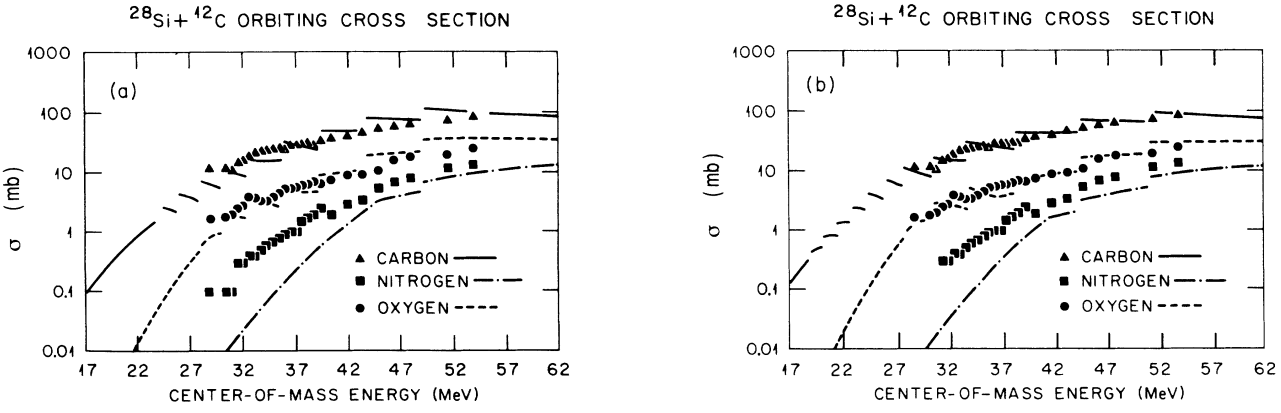

FIG. 4. (a) Measured and calculated (with set I) orbiting cross sections for C, N, and O channels in Si+C collisions plotted as functions of bombarding energy. (b) As in part (a), but with parameter set II.

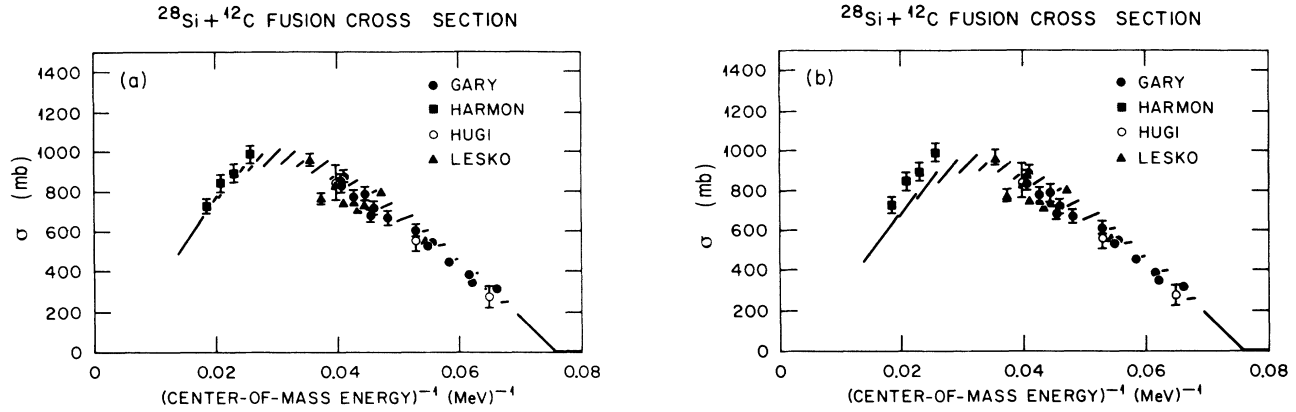

FIG. 5. (a) Measured and calculated (with set I) fusion cross section in Si+C collisions plotted as functions of inverse of the bombarding energy. (b) As in part (a), but with parameter set II.

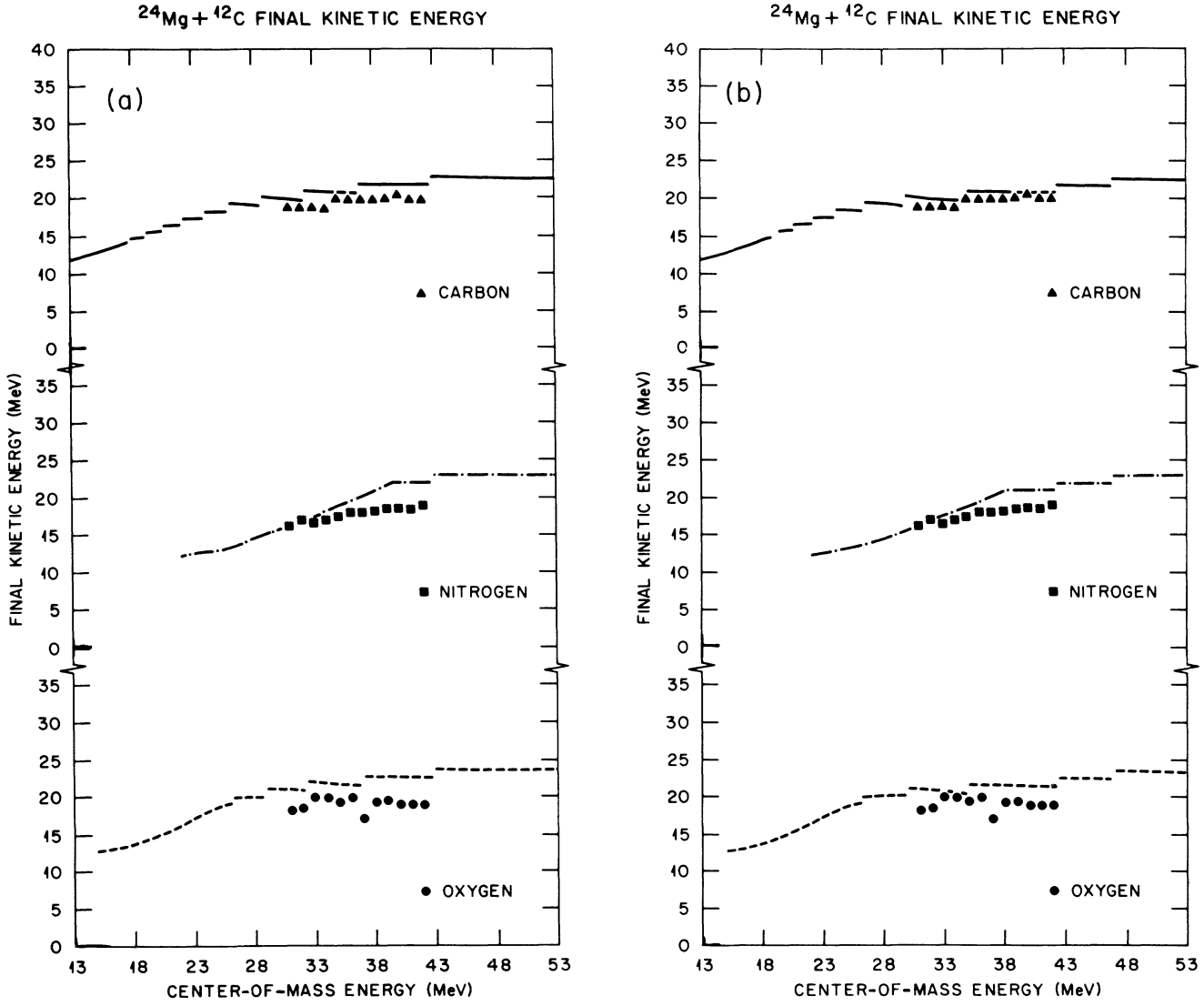

FIG. 6 (a) Measured and calculated (with set I) final kinetic energies of C, N, and O channels in Mg+C collisions plotted as functions of bombarding energy. (b) As in part (a), but with parameter set II.

nels over a broad range of bombarding energies. In Fig. 4, the orbiting cross section for the channels C+Si, N+Al, and O+Mg are plotted as a function of bombarding energy and compared with data. Parts (a) and (b) of the figure show the results of calculations done by set I and set II, respectively. Calculations reproduce the orbiting cross section for the two strongest channels surprisingly well, but the yield for the N channel is underpredicted. The available excitation energy in the N channel is much smaller than the stronger channels. At low excitation energies Fermi gas expression with global level density parameters does not work very well and produces low yield for the N channel. In order to improve the calculations at low energies, a more accurate description of level densities is required. In Fig. 5, the fusion cross section is plotted as a function of bombarding energy and compared with data. Both calculations done with set I in part (a) and with set II in part (b) describe the trend seen in data over a large range of bombarding energy, saturation, and decrease in fusion cross section are correctly reproduced. However, the parameter set I provides a better overall description than set II.

As a second application of the model, we consider the collision of Mg+C nuclei. We employ the same parameter sets in the calculations as for the Si+C system. Figures 6–8 show a comparison of the results of calculations with the experimental data. Calculations with either set of parameters provide a good description for the final kinetic energies of the orbiting products and for the orbiting cross sections over a wide range of bombarding energies. The fits can be improved by adjusting the strengths parameter A of the Bass potential, however this is not done here. The measured cross sections for the O channel are larger than predicted by the calculation, because of contributions from the α+O decay of excited states in Ne populated in the Ne+O channel. As seen in Fig. 8, the calculated fusion cross section deviates from data at higher bombarding energies. Calculated cross section saturates around $E \cong 30$ MeV and decreases for increased energies, whereas the data increase steadily. The data measured at Saclay,[20] though, show a tendency to decrease at higher energies. These measurements were done with a Mg beam and provided a better separation of fusion from other strongly damped processes.

As a third application, we consider the collision of the Si+N system. For this system, in order to produce the

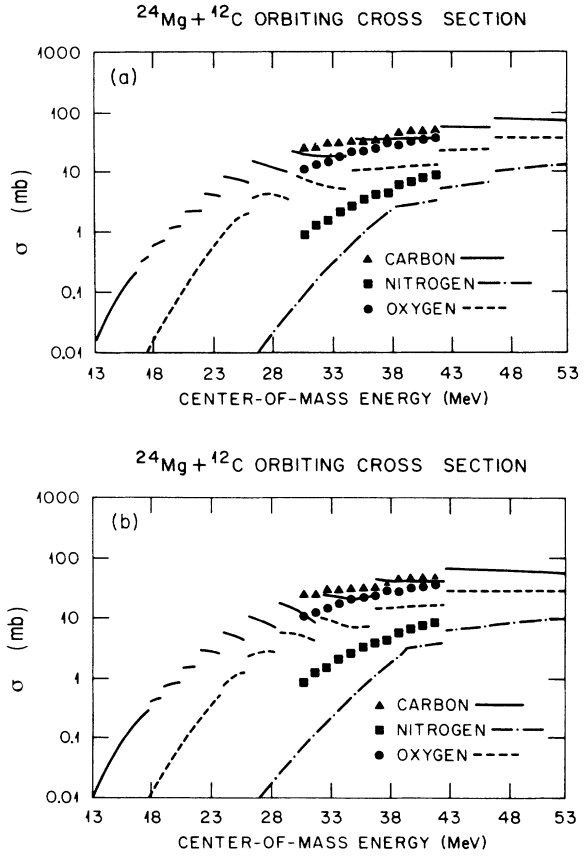

FIG 7. (a) Measured and calculated (with set I) orbiting cross section for C, N, and O channels in Mg+C collisions plotted as functions of bombarding energy. (b) As in part (a), but with parameter set II.

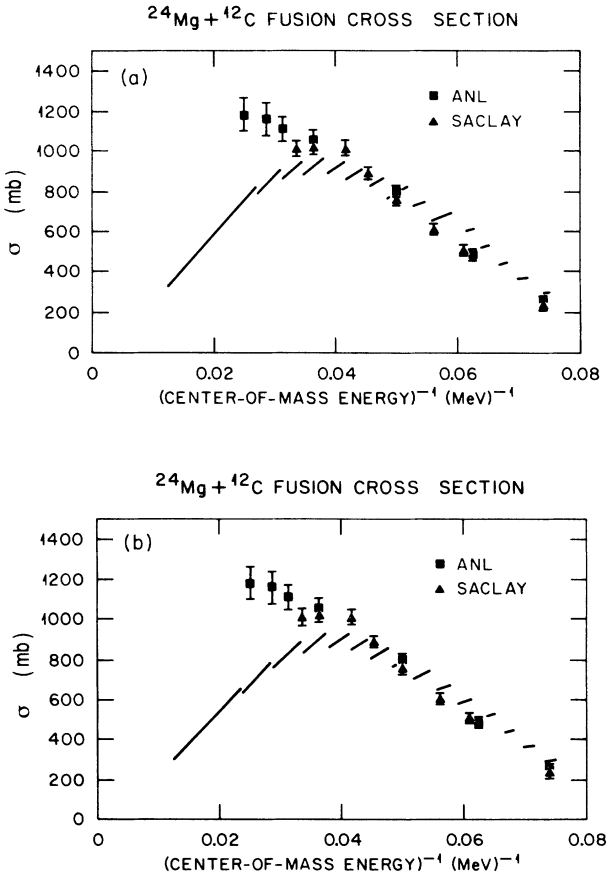

FIG. 8. (a) Measured and calculated (set I) fusion cross sections in Mg+C collisions plotted as functions of bombarding energy. (b) As in part (a), but with parameter set II.

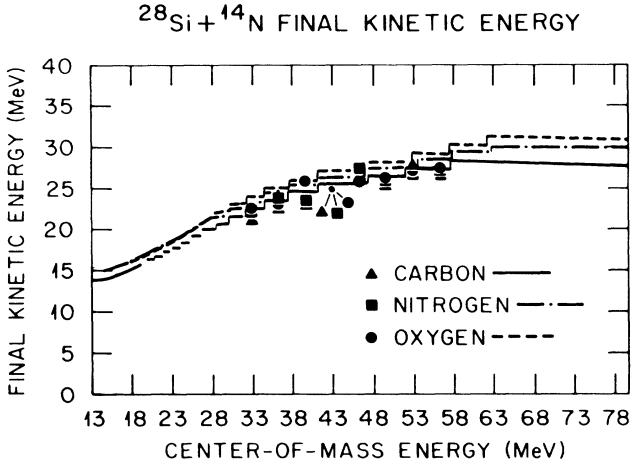

FIG. 9. Measured and calculated (with set III) final kinetic energies of C, N, and O channels in Si+N collisions plotted as functions of bombarding energy.

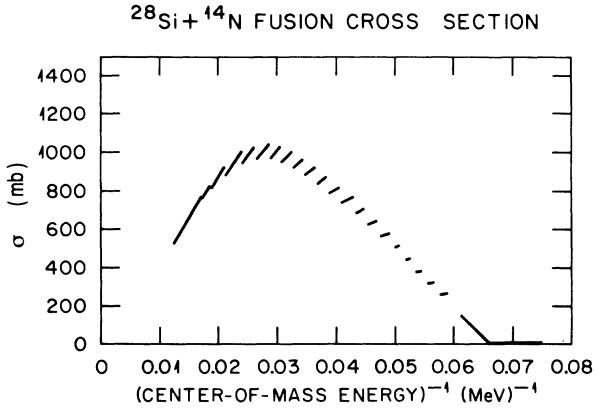

FIG. 11. Calculated (with set III) fusion cross section in Si+N collision plotted as a function of bombarding energy.

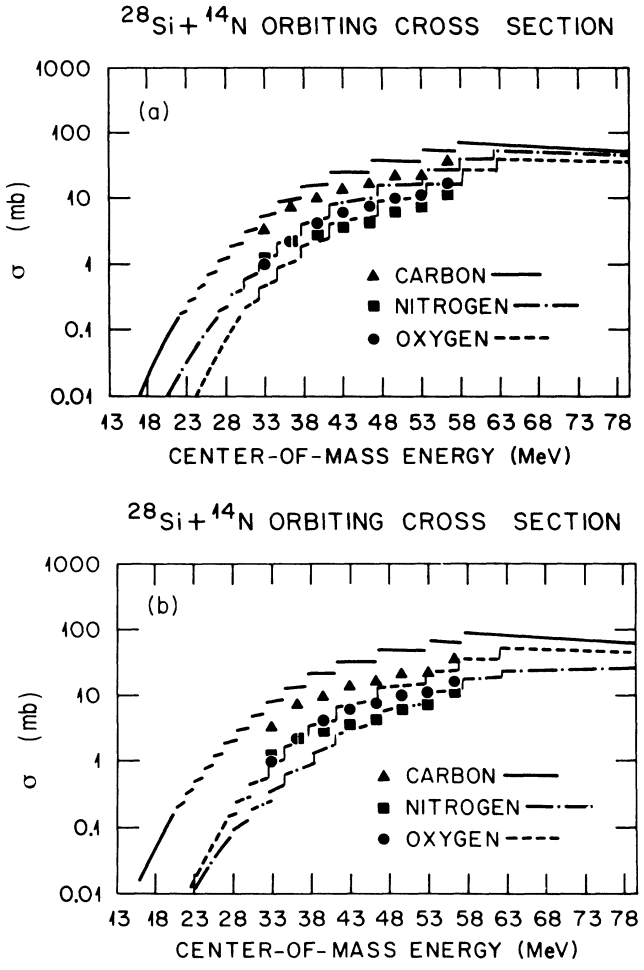

FIG. 10. (a) Measured and calculated orbiting cross section for C, N, and O channels in Si+N collisions plotted as functions of bombarding energy. Calculation using mass weighted mean of pairing energy. (b) As in part (a), but with parameter set III using pairing energy of heavier partner.

final kinetic energies of emitted fragments, the strength parameter A is slightly adjusted and taken to be $A=0.040$ (set III) and the other parameters remain fixed to their original values. Figures 9–11 show the results of calculations and comparison with the experimental data except the fusion cross section for which experimental data are not available. As seen from Figs. 9 and 10, the calculations produce a reasonable description, as for the previous cases, for the kinetical energies of the emitted fragments and for the orbiting cross sections of C, N, and O channels over a wide range of bombarding energies. Both experimental and calculated orbiting yields for N and O channels are very close to each other, within a few millibarns. Small fluctuations in the orbiting yield are very sensitive to the parameters of the Fermi gas level density and with global parameters it is very difficult to reproduce the correct ordering of the orbiting yield in N and O channels. In order to illustrate this point, we use two different prescriptions[8] to calculate pairing energies of dinuclear couples: (i) pairing energy of DMC is approximated by the mass weighted mean pairing energy of binary fragments and (ii) pairing energy of DMC is approximated by the pairing energy of the heavier partner. Figure 10(a) shows the result of calculations with the mean pairing energies. This prescription does not give the correct ordering and produces slightly higher yield in the N channel than the O channel. Figure 10(b) shows the result of calculations with the pairing energies of heavier partners, which produce the correct ordering for the yields in N and O channels.

V. SUMMARY AND CONCLUSIONS

We develop a transport description for the capture processes in low-energy nuclear collisions. As a result of the action of dissipative forces on relative motion, it is assumed that the colliding ions are trapped into the pocket of entrance channel nucleus-nucleus potential, and a dinuclear molecular complex is formed. It acts as a doorway configuration toward formation of a fully equilibrated compound nuclei. At each stage of evolution, the

DMC can decay into open binary channels by dynamical and thermal penetration over the interaction barrier. Assuming a random matrix model for the relevant coupling matrix elements, the evolution of the DMC and the fragmentation into binary exit channels are described by two coupled transport equations. The formalism provides a consistent description for the intermediate processes (orbiting and fast fission) and for the compound nucleus formation, including the effects of the entrance channel limitations.

The formalism is applied to analyze the orbiting and fusion processes in the collision of light systems. A further approximation is introduced by assuming that the DMC remains close to a local equilibrium with respect to the mass-asymmetry mode. As a result, the binary fragmentation probability is determined by the available phase space of the DMC and it can be calculated in terms of the density of states and the potential energy surface of the system. In the calculations, we employ the Fermi gas expression for the density of states and a potential energy surface in which the nuclear part is determined by a one-dimensional Bass proximity potential. The model provides a remarkably good description for the orbiting and fusion processes observed in the collisions of Si+C, Si+N, and Mg+C systems.

ACKNOWLEDGMENTS

The authors would like to thank M. Prahovic for his help in the calculations. One of us (S.A.) is grateful to the Physics Division, Oak Ridge National Laboratory, for their support. Oak Ridge National Laboratory is operated by Martin Marietta Energy Systems, Inc. under Contract DE-AC05-84OR21400 with the U.S. Department of Energy. The A. W. Wright Nuclear Structure Laboratory is supported through Contact DE-AC02-76ER03074 with the U.S. Department of Energy.

[1]J. R. Birkelund *et al.*, Phys. Rep. **56**, 107 (1979); Annu. Rev. Nucl. Part. Sci. **33**, 265 (1981).
[2]J. R. Huizenga and U. W. Schroeder, in *Treatise on Heavy Ion Science,* edited by D. A. Bromley (Plenum, New York, 1984), Vol. 2.
[3]R. Vandenbosch *et al.*, Nucl. Phys. **A339**, 167 (1980).
[4]A. Gobbi and W. Norenberg, in *Heavy Ion Collisions,* edited by R. Bock (North-Holland, Amsterdam, 1980), Vol. 2.
[5]C. Ngo *et al.*, Nucl. Phys. **A400**, 259 (1983).
[6]J. Toke *et al.*, Nucl. Phys. **A440**, 327 (1985).
[7]D. Shapira *et al.*, Phys. Lett. **114B**, 111 (1982); Phys. Rev. Lett. **53**, 1634 (1984).
[8]B. Shivakumar *et al.*, Phys. Rev. Lett. **57**, 1211 (1986); Phys. Rev. C **37**, 652 (1988).
[9]W. Norenberg, Phys. Lett. **53B**, 289 (1974).
[10]S. Ayik *et al.*, Z. Phys. A **277**, 299 (1976); **279**, 145 (1976); **297**, 55 (1980).
[11]S. Ayik and W. Norenberg, Z. Phys. A **288**, 401 (1978); **297**, 55 (1980).
[12]H. A. Weidenmuller, Prog. Nucl. Part. Phys. **3**, 49 (1980).
[13]J. Randrup, Nucl. Phys. **A307**, 319 (1978); **A327**, 490 (1979).
[14]H. Feldmeier and H. Spangenberger, Nucl. Phys. **A428**, 223 (1984); **A435**, 229 (1985).
[15]B. Shivakumar, S. Ayik, B. A. Harmon, and D. Shapira, Phys. Rev. C **35**, 1730 (1987).
[16]G. J. Mathews and L. G. Moretto, Phys. Lett. **87B**, 331 (1979).
[17]M. S. Hussein *et al.*, Phys. Rev. Lett. **54**, 2659 (1985).
[18]M. Hugi *et al.*, Nucl. Phys. **A368**, 173 (1981).
[19]K. T. Lesko *et al.*, Phys. Rev. C **25**, 872 (1982).
[20]S. Gary and C. Volant, Phys. Rev. C **25**, 1877 (1982).
[21]B. A. Harmon *et al.*, Phys. Rev. C **34**, 552 (1986).
[22]A. W. Dunnweber *et al.*, Phys. Rev. Lett. **61**, 927 (1988).
[23]A. Glaesner *et al.* (unpublished).
[24]C. Mahaux and H. A. Wedenmuller, *Shell-Model Approach to Nuclear Reactions* (North-Holland, Amsterdam, 1969).
[25]R. Bass, Phys. Rev. Lett. **39**, 265 (1977).
[26]J. Wilczyanski and K. Siwek-Wilczyska, Phys. Lett. **55B**, 270 (1975).
[27]A. Bohr and B. R. Mottelson, *Nuclear Structure* (Benjamin, New York, 1969), Vol. 1, p. 281.